Influence of junction temperature on chromaticity and color-rendering properties of trichromatic white-light sources based on light-emitting diodes

S. Chhajed
Department of Electrical, Computer, and Systems Engineering, Rensselaer Polytechnic Institute, Troy, New York 12180

Y. Xi
Department of Physics, Applied Physics, and Astronomy, Rensselaer Polytechnic Institute, Troy, New York 12180

Y.-L. Li and Th. Gessmann
Department of Electrical, Computer, and Systems Engineering, Rensselaer Polytechnic Institute, Troy, New York 12180

E. F. Schubert[a]
Department of Electrical, Computer, and Systems Engineering and Department of Physics, Applied Physics, and Astronomy, Rensselaer Polytechnic Institute, Troy, New York 12180

Trichromatic white-light sources based on light-emitting diodes (LEDs) offer a high luminous efficacy of radiation, a broad range of color temperatures and excellent color-rendering properties with color-rendering indices (CRIs) exceeding 85. An analysis of the luminous efficacy and CRI of a trichromatic light source is performed for a very broad range of wavelength combinations. The peak emission wavelength, spectral width, and the output power of LEDs strongly depend on temperature and the dependencies for red, green, and blue LEDs are established. A detailed analysis of the temperature dependence of trichromatic white LED sources reveals that the luminous efficacy decreases, the color temperature increases, the CRI decreases and the chromaticity point shifts towards the blue as the junction temperature increases. A high CRI > 80 can be maintained, by adjusting the LED power ratio so that the chromaticity point is conserved. © *2005 American Institute of Physics*. [DOI: 10.1063/1.1852073]

I. INTRODUCTION

Solid-state lighting technology, due to advantages such as high efficiency and long life, is believed to replace conventional, inherently less efficient incandescent and fluorescent light sources.[1–3] It is well established that semiconductor-based light sources have, in principle, the potential of achieving near 100% power efficiency. State-of-the-art light-emitting diodes (LEDs) are already being used in numerous applications such as traffic signals and full-color video displays,[4] and it is expected that LEDs will be increasingly used in general lighting applications.

However, the requirements for general lighting differ from those of other applications. *First*, the color-rendering index (CRI) of the light source, defined as the ability of the light source to render the true colors of an object, should be high. The maximum value of the CRI is 100, which implies the best possible color rendition. *Second*, the luminous efficacy (LE) and the luminous efficiency, both measured in lumens per watt (lm/W), are important performance criteria for white-light sources. The luminous efficacy of radiation is the efficiency of conversion from optical power to luminous flux. The luminous efficiency of the source is the ratio of luminous flux to the input electrical power. The highest LE is obtained for a monochromatic emission at 555 nm, where the human eye is most sensitive.[5] However, the CRI of such

a monochromatic source would be poor. As is well known, there is a fundamental tradeoff between CRI and LE, that is, one of the two quantities can be maximized only at the expense of the other.

LEDs inherently have narrow emission linewidths as compared to phosphors and incandescent sources, and therefore pose a challenge for the generation of white light. There are two different approaches for producing white light using LEDs.[6,7] In the first approach, which employs phosphors, partial down-conversion of high-energy photons (<460 nm) to lower energy photons, takes place in the phosphor. This type of approach has the advantage of a compact package, a single power supply, and a high CRI due to the broad emission spectrum of a phosphor.[8] The approach also has great color stability, in particular if a UV source is used to excite the phosphor. However, phosphor-based sources suffer from limited LE due to down-conversion (Stokes shift) and relatively broad emission spectra.

The Stokes shift energy loss is unavoidable and cannot be overcome in conventional phosphor materials. The Stokes energy loss incurred during conversion of a photon of wavelength λ_1 to a photon of wavelength λ_2 ($\lambda_1 < \lambda_2$) is given by

$$\Delta E = h\nu_1 - h\nu_2 = \left(\frac{hc}{\lambda_1}\right) - \left(\frac{hc}{\lambda_2}\right), \tag{1}$$

where h is Planck's constant and c is the speed of light in vacuum.

[a]Author to whom correspondence should be addressed; electronic mail: efschubert@rpi.edu
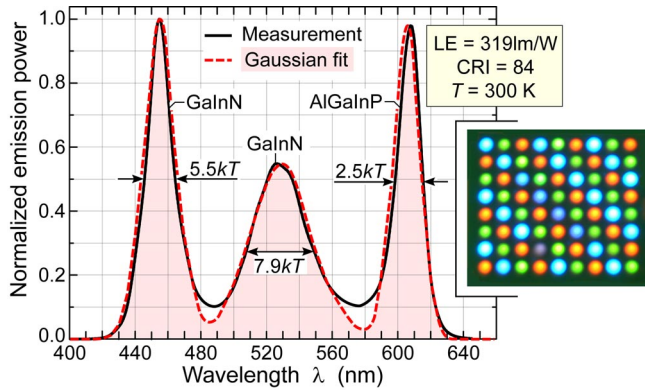
FIG. 1. (Color online) Experimental emission spectrum of trichromatic LED-based white-light source with $T_C = 6500$ K (solid line) and Gaussian fit (dashed line). The inset shows a photograph of the trichromatic light source.

Thus, the energy efficiency of a wavelength converter is given by

$$\eta_{h\nu} = 1 - \frac{h\nu_1 - h\nu_2}{h\nu_1} = \frac{\lambda_1}{\lambda_2}. \qquad (2)$$

In the second approach, emission from multiple single-color LEDs is additively mixed to generate white light. Since there is no loss due to the down-conversion, this approach offers white light sources with potentially very high luminous efficiency. Theoretically dichromatic white-light

sources are most efficient, offering an efficacy of >440 lm/W.[9] However, the CRI of dichromatic sources is low. The CRI can be improved dramatically by increasing the number of primary-color LEDs for a white source. However, sources with a greater number of primary-color LEDs have lower LE.

Trichromatic LED-based white-light sources achieve an excellent balance between CRI and LE.[10] CRI exceeding 85 and LE in excess of 300 lm/W can be obtained with the optimum combination of wavelengths.

In this article, comprehensive data for the LE and CRI of a trichromatic light source are provided for a very broad range of wavelength combinations. The temperature dependences of the LED peak wavelength, spectral width, and output power are determined experimentally. The changes in LE, correlated color temperature (CCT), CRI, and chromaticity coordinates are determined. These parameters change drastically with temperature and can render the source unsuitable for certain applications. It is shown that this problem can be alleviated by changing the power ratio of the individual LEDs, thereby maintaining the CRI and luminous efficacy of the source at high values.

II. TRICHROMATIC LED-BASED WHITE LIGHT SOURCE

A trichromatic LED-based white light source can be formed by assembling GaInN blue and green LEDs and Al-
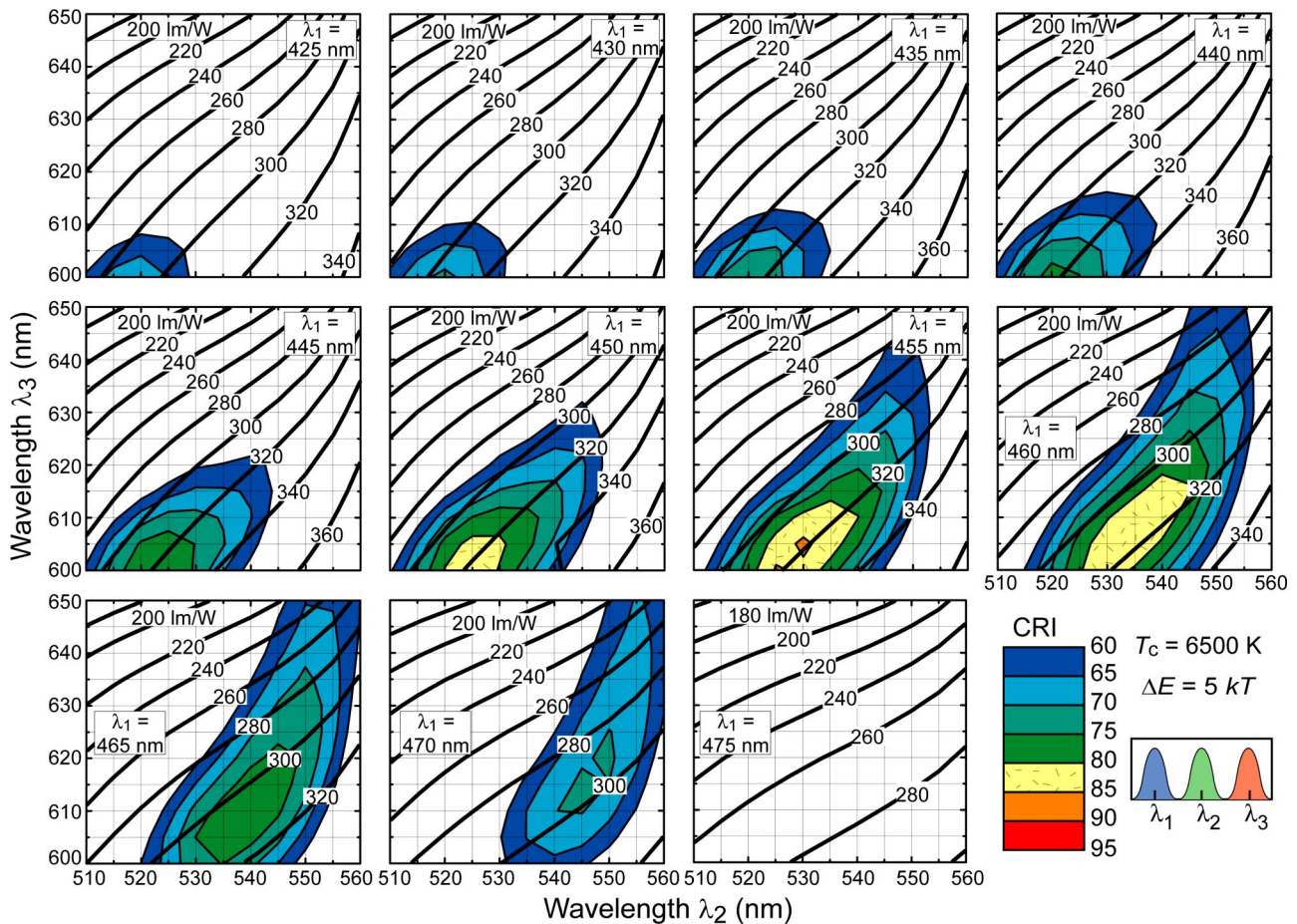

FIG. 2. (Color online) Contour plots showing LE of radiation and CRI of a trichromatic gaussian white-light source with linewidth of 5 kT at 300 K for different wavelength combinations.
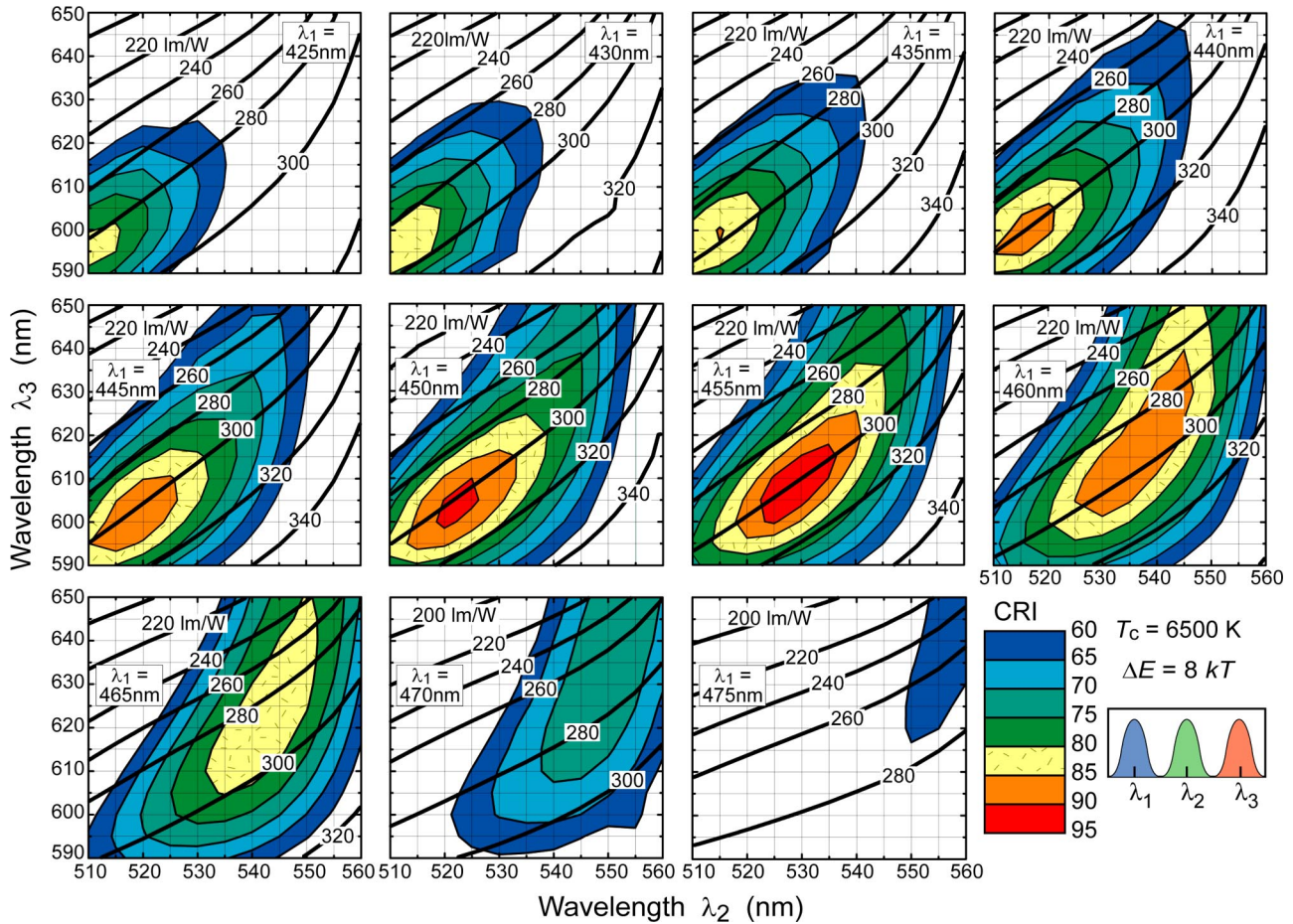
FIG. 3. (Color online) Contour plots showing LE of radiation and CRI of a trichromatic gaussian white-light source with linewidth of 8 kT at 300 K for different wavelength combinations.

GaInP red LED in an array. Figure 1 shows the experimental emission spectrum of such a white-light source (solid line) consisting of 72 devices. The figure also shows a Gaussian fit (dashed line) to the experimental spectrum. We can see that the Gaussian closely matches the experimental spectrum. The power ratio of the LEDs is adjusted to obtain a chromaticity point on Planckian locus with a color temperature of 6500 K. The inset shows the photograph of the light source. The experimental spectra display a linewidth [full width at half-maximum (FWHM)] of 5–8 kT. The linewidths are more than the theoretically expected linewidth of 1.8 kT, which originates in thermal broadening effects. Giving the linewidths in terms of units of kT is very useful as it allows for convenient comparison with the theoretical linewidth of 1.8 kT. The additional line broadening found in the experimental emission spectra can be attributed to alloy broadening, that is, the statistical fluctuation of the active region alloy composition. As can be seen from Fig. 1, alloy broadening is particularly strong in the case of GaInN LEDs, possibly due to InN phase separation.

To determine the best possible wavelength combination for a trichromatic source, LE and CRI for a wide range of wavelength combinations are calculated from Gaussian fits to experimental spectra. The CRI is calculated using the procedure detailed by CIE.[11] Figure 2 shows the contour plots of LE and CRI for a large combination of wavelengths. The

linewidth is assumed to be 5 kT, which is comparable to the blue emitter, but narrower than the green and broader than the red emitter. For $\Delta E = 5$ kT, LE as high as 318 lm/W and CRI as good as 86 can be obtained with a wavelength combination of $\lambda_1 = 455$ nm, $\lambda_2 = 530$ nm, $\lambda_3 = 605$ nm.

Figure 3 shows the contour plots of LE and CRI for various wavelength combinations assuming a linewidth of 8 kT. The highest LE values and the best color-rendering properties are found for the wavelength combination of $\lambda_1 = 455$ nm, $\lambda_2 = 530$ nm, $\lambda_3 = 610$ nm. The LE for this wavelength combination is 300 lm/W and the CRI is 93. These values of the LE and the CRI are suited even for the most demanding illumination applications and they are far superior to the typical LEs of incandescent lamps.

Comparison of Figs. 2 and 3 shows the fundamental trade-off between luminous efficacy and CRI. As the linewidth changes from 5 to 8 kT, the LE decreases and CRI increases for the same wavelength combination. The results in Figs. 2 and 3 show that both, high LE and good CRI can be obtained by trichromatic LED-based white-light sources. As can be inferred from these figures, the CRI values of such sources decrease rapidly for even small deviations in wavelengths from the optimum values. We observe, in Fig. 2, that for an increase of just 20 nm in any one of the three optimum wavelengths the CRI decreases from 86 to <60. Therefore,

maintaining the optimum values of wavelengths is very important for producing high LE and CRI white light.

However, the junction temperature of the LED strongly affects the peak wavelength, spectral width, and output power. Each of these factors affects the LE and CRI of the light source. The junction temperature and the temperature coefficients of LED parameters (peak wavelength, spectral width, and power) are therefore of critical importance, and a detailed analysis of these parameters will be presented next.

III. MEASUREMENT OF JUNCTION TEMPERATURE

The junction temperature of an LED affects peak wavelength, spectral width, output power, internal efficiency, maximum output power, reliability, and lifetime, etc. Different techniques, such as micro-Raman spectroscopy, electroluminescence, photoluminescence, thermal resistance, and threshold voltage, have been used to determine the junction temperature.[12–14] In this article, the junction temperature of red, green, blue, and UV LED is measured using three different methods namely by the forward-voltage, peak-wavelength-shift, and high-energy-slope method.

The forward-voltage method[15] consists of two parts. The first part is a pulsed calibration measurement and the second part is a dc measurement. In the calibration measurement, a pulsed current of duty cycle of 0.1% (10 to 100 mA in steps of 10 mA) is passed through the LED mounted inside an oven with controlled temperature. It is very reasonable to assume that the junction temperature of the LED is the same as the oven temperature because no significant heating is caused by the pulsed current of very low duty cycle. The forward-voltage drop is recorded using a multimeter for different values of the pulsed current at temperatures ranging from room temperature to 120 °C in steps of 20 °C. The calibration measurement establishes the relationship between the forward voltage V_f and the junction temperature T_j. In the second part, dc current is passed through the LED kept in room-temperature ambient. The forward-voltage drop is recorded at current levels ranging from 10 to 100 mA in steps of 10 mA. The calibration measurement serves as the reference for the derivation of the junction temperature from the dc measurement. The forward voltage recorded during the dc measurement is used to determine the junction temperature using the calibration plots. Figure 4 shows the calibration plots for the forward-voltage method. An approximately linear decrease in V_f with respect to T_j is observed.

The change in band gap energy with temperature is used in the peak-wavelength-shift method. A similar procedure, that is, pulsed calibration and the dc measurement, is used. The peak wavelength is recorded for each temperature of the calibration measurement using an optical spectrum analyzer.

Figure 5 shows the calibration plots for the peak-wavelength-shift method. We notice that the peak wavelength of III-V nitride-based LEDs shifts towards shorter wavelengths with increasing drive current even when the temperature is maintained constant. This short-wavelength shift is not observed in the case of III-V phosphide-based red LEDs. This blueshift in case of the III-V nitride-based LEDs is due to the piezoelectricity-induced quantum confined Stark
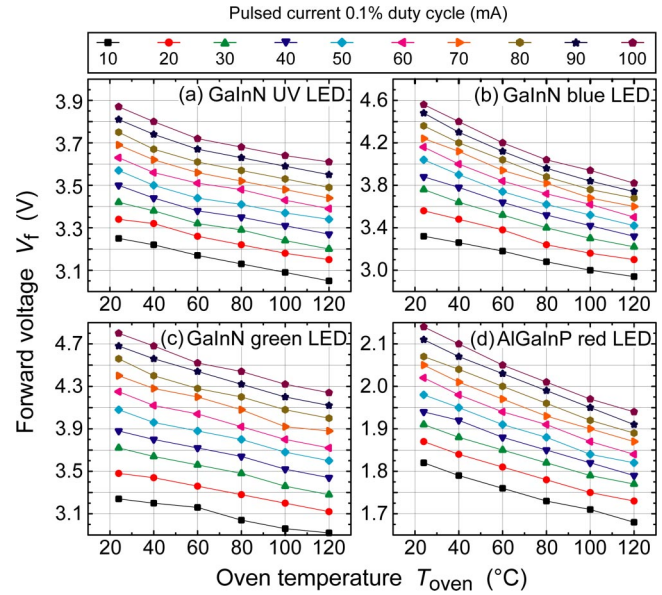

FIG. 4. (Color online) Calibration curves of forward voltage vs oven temperature for UV, blue, green, and red LEDs at different values of the pulsed current.

effect.[16] Note that the redshift in the peak wavelength of the red AlGaInP LED is greater than that of the blue and green LED. Table I lists the temperature coefficients of peak wavelength, spectral width for blue, green, and red LEDs.

In the high-energy slope method, spectra of LEDs are recorded at different current levels. Assuming the Boltzmann distribution, the intensity can be described by

$$I \propto \exp\left(-\frac{h\nu}{kT}\right), \tag{3}$$

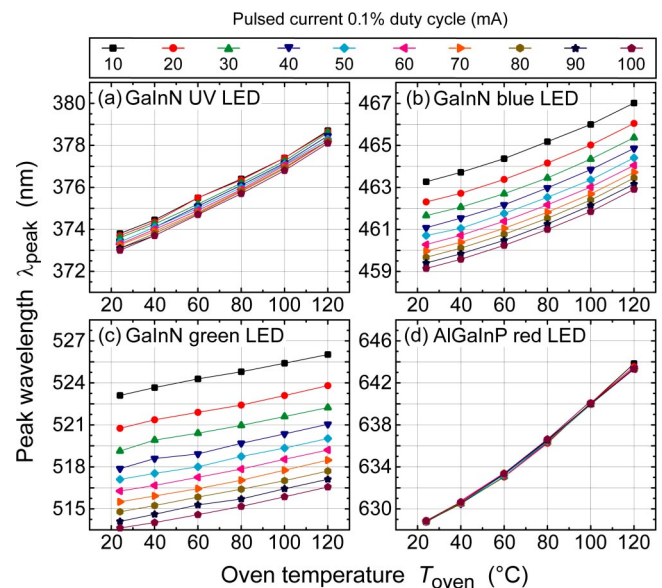where k is the Boltzmann constant and T is the carrier temperature.

FIG. 5. (Color online) Calibration curves of peak wavelength vs oven temperature for UV, blue, green, and red LEDs at different values of the pulsed current. The separation in the curves corresponding to different values of current in case of III-V nitride UV, blue, and green LEDs is due to the quantum confined Stark effect.

TABLE I. Experimentally determined temperature coefficients of various LED parameters.

	$d\lambda_{peak}/dT$ (nm/°C)	$d\Delta\lambda/dT$ (nm/°C)	T_{char} (K)
Blue	0.0389	0.0466	493
Green	0.0308	0.0625	379
Red	0.1562	0.1812	209

Therefore, we can deduce the carrier temperature from the slope of the high-energy part of the spectrum. This carrier temperature is generally higher than the actual junction temperature. Figure 6 shows the spectra and carrier temperatures of a blue GaInN LED for dc current values of 20 and 100 mA. Note the increase in carrier temperature at higher dc current. Data from the region near the peak but on the high-energy side are used for the measurement of the carrier temperature because at even higher energies, the optical signal is very weak.

Figure 7 shows the results of all three methods of junction temperature measurement for UV, blue, green, and red LEDs. The results from the first two methods, forward-voltage and peak-wavelength-shift, are in good agreement with each other. The uncertainty in the junction temperature measurement by the peak-wavelength-shift method is higher due to the uncertainty involved with measurement of the peak wavelength. It is generally accepted that the accuracy in the peak position of an emission line is $1/10$ of the linewidth (FWHM). Therefore, we conclude that the forward-voltage method provides the most accurate values of the LED junction temperature. We estimate the accuracy of the forward-voltage method to be ± 3 °C. The temperatures obtained from the high-energy-slope method are much higher than the actual value of the junction temperature.

In the experiments just presented, the device output power is recorded. The temperature dependence of the output power can be described by

$$I = I_0|_{300\ \mathrm{K}} e^{-(T-300\ \mathrm{K})/T_{char}}, \tag{4}$$

where T_{char} is called the characteristic temperature.
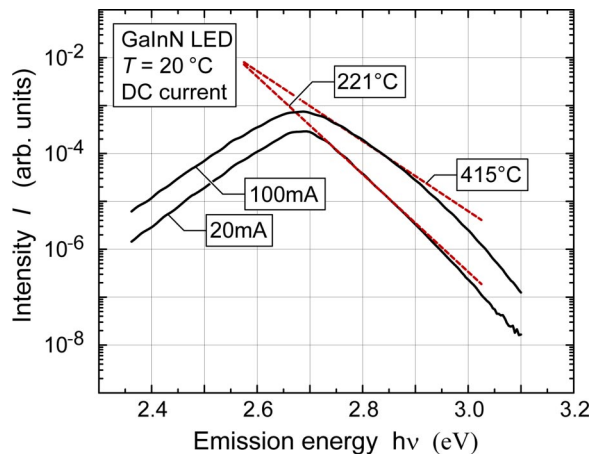

FIG. 6. (Color online) Electroluminescence spectra of GaInN blue LED at 20 and 100 mA. Dashed lines represent the linear fit to the high-energy side of the spectrum, where carrier distribution can be approximated by the Boltzmann distribution.
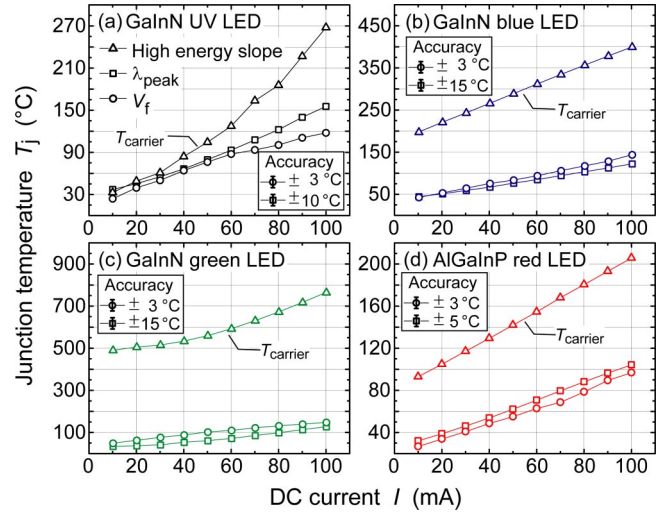

FIG. 7. (Color online) Plots of junction temperature vs dc current for UV, blue, green, and red LEDs. The forward-voltage method is most accurate. The high-energy-slope method gives us the carrier temperature.

Experimentally determined values of temperature coefficients of peak wavelength, FWHM, and characteristic temperatures for different LEDs are shown in Table I. Note that all LEDs show a redshift of the spectrum with increasing temperature.

IV. LE AND CRI AS A FUNCTION OF TEMPERATURE

Theoretically, a spectral width of 1.8 kT is expected for the thermally broadened emission. However, due to other broadening mechanisms, such as alloy broadening, the observed values of spectral width at room temperature in III-V nitride LEDs are 5–8 kT. This broadening in the emission spectrum results in a small movement of the chromaticity point away from the perimeter towards the center of the chromaticity diagram.

Experimental evidence discussed earlier supports the use of the Gaussian function to describe the spectral power density function of an LED. Therefore,

$$P(\lambda) = P \frac{1}{\sigma\sqrt{2\pi}} \exp\left[-\frac{1}{2}\left(\frac{\lambda - \lambda_{peak}}{\sigma}\right)^2\right], \tag{5}$$

where

$$\sigma = \frac{\lambda_{peak}^2 \Delta E}{2hc\sqrt{2\ln 2}}, \tag{6}$$

where ΔE is the FWHM of the emission spectrum and P is the optical power of the LED.

Therefore the spectral power density function for the trichromatic LED-based white-light source can be given as

$$P_{white}(\lambda) = P_{blue}(\lambda) + P_{green}(\lambda) + P_{red}(\lambda). \tag{7}$$

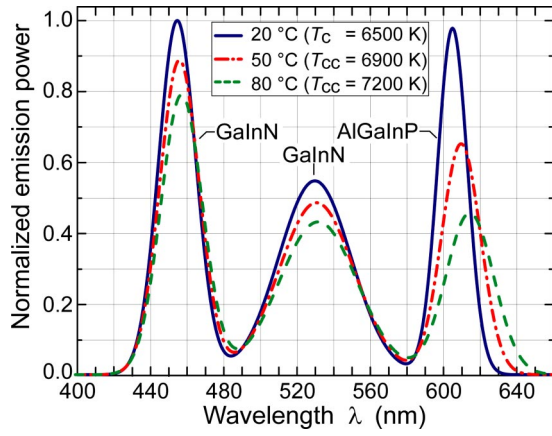The LE of this source can be calculated using

FIG. 8. (Color online) Emission spectrum for a trichromatic LED-based white-light source at different junction temperatures. The optical power ratio of the LEDs is constant so that the color temperature/CCT of the light source changes.

$$\text{LE} = \frac{\left(683\frac{\text{lm}}{\text{W}}\right)\int_\lambda P_{\text{white}}(\lambda)V(\lambda)d\lambda}{\int_\lambda P_{\text{white}}(\lambda)d\lambda}, \tag{8}$$

where $V(\lambda)$ is the eye sensitivity function.

To calculate the CRI of the trichromatic LED-based white-light source, the CIE 1976 (u',v') uniform chromaticity coordinates are used. The reference light source chosen is
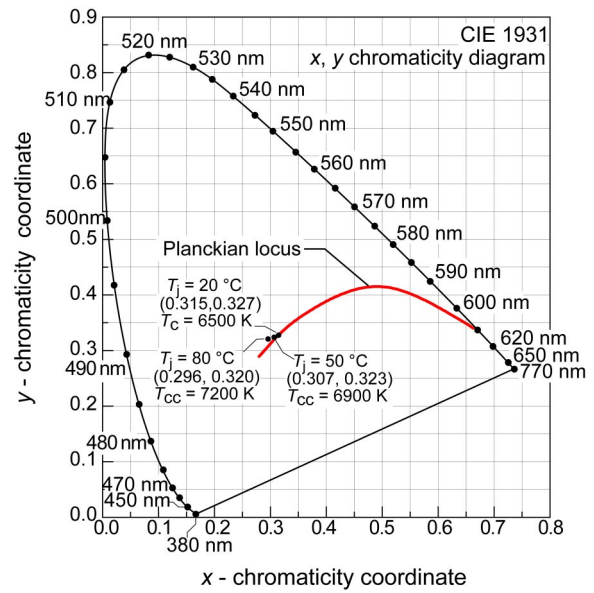

FIG. 9. (Color online) Chromaticity point of a trichromatic LED-based white-light source for different junction temperatures.

a Planckian radiator with color temperature of 6500 K. The calculation procedure defined by CIE[11] is followed. An adaptive color shift is taken into account for CRI calculations for $T_j=50$ and 80 °C, where the chromaticity coordinates of the trichromatic LED-based white-light source move away from the Planckian locus.

TABLE II. Peak wavelength, spectral width, and power ratios of individual LEDs for different values of junction temperature. Also given are the calculated values of the CRI and LE.

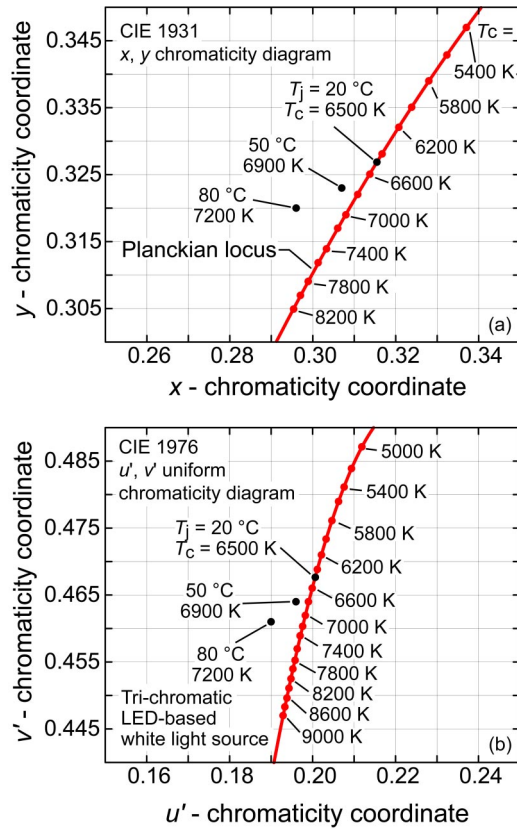| 20 °C | λ_{peak} (nm) | 455 | 530 | 605 | $(x,y)=(0.315,0.327)$ |
	$\Delta\lambda$ (nm)	23.9	46.6	19.2	CRI=84
	ΔE (kT)	5.5	7.9	2.5	LE=319 lm/W
	P_{int} (W)	1	1.067	0.786	T_C=6500 K
50 °C	λ_{peak} (nm)	456.2	530.9	609.7	$(x,y)=(0.307,0.323)$
	$\Delta\lambda$ (nm)	25.3	48.5	24.64	T_{CC}=6900 K
	ΔE (kT)	5.8	8.2	3.2	CRI=80
	P_{int} (before power adjustment) (W)	0.941	0.986	0.681	LE=307 lm/W
					Changing power ratio
					T_C=6500 K
					CRI=85
	P_{int} (after power adjustment) (W)	1	1.08	0.801	LE=311 lm/W
80 °C	λ_{peak} (nm)	457.4	531.8	614.4	$(x,y)=(0.296,0.320)$
	$\Delta\lambda$ (nm)	26.7	50.4	30.08	T_{CC}=7200 K
	ΔE (kT)	6.1	8.5	3.9	CRI=72
	P_{int} (before power adjustment) (W)	0.885	0.911	0.590	LF=297 lm/W
					Changing power ratio
					T_C=6500 K
					CRI=81
	P_{int} (after power adjustment) (W)	1	1.079	0.834	LF=302 lm/W

FIG. 10. (Color online) Chromaticity point of a trichromatic LED-based white-light source for different junction temperatures.
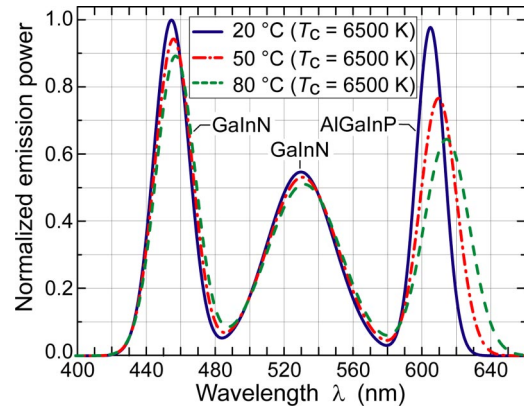

FIG. 11. (Color online) Emission spectrum for trichromatic LED white-light source with different junction temperatures. Note that the optical power ratio is adjusted so that the color temperature and the chromaticity coordinates are not changed.

The spectra of the white source after such power adjustment at $T_j=50$ and 80 °C are shown in Fig. 11. With such power adjustment, it is shown that, the LE and CRI can be maintained above 300 lm/W and 80, respectively.

V. CONCLUSION

In conclusion, experimental results and calculations show that trichromatic LED-based white-light sources are illumination sources with excellent CRI and LE suitable even for the most demanding illumination applications. An analysis of the LE and CRI of a trichromatic light source is performed for a very broad range of wavelength combinations. Detailed experiments are performed to establish the junction temperature dependence of peak wavelength, spectral width, and output optical power. It is observed that the chromaticity point shifts, CRI decreases (84 to 72), color temperature increases (6500 to 7200 K) and the LE decreases (319 to 297 lm/W) as the junction temperature increases from 20 to 80 °C. The change in CRI caused with increasing junction temperature can be problematic for certain applications. Therefore the ability to tune the source by changing the input electrical power of individual LEDs is required so as to maintain the chromaticity coordinates, CRI, and LE at acceptable values. A high CRI >80 and LE >300 lm/W can be maintained, if the chromaticity point is conserved by power adjustment of the individual LEDs.

ACKNOWLEDGMENTS

The change in LED parameters results in a change in the spectrum of the trichromatic white source, as shown in Fig. 8. The values of the temperature coefficients of the peak wavelength, spectral width, and the characteristic temperature, listed in Table II, are used to calculate the LE. CRI, color temperature, and chromaticity coordinates at $T_j=20$, 50, and 80 °C. The movement of the chromaticity point with junction temperature is shown in Fig. 9. Notice that the chromaticity point moves towards higher color temperatures owing to the strong decrease in intensity of the red LED. Figure 10 shows the chromaticity coordinates of the white-light source at $T_j=20$, 50, and 80 °C along with the Planckian locus in the CIE 1931 x-y chromaticity coordinate system as well as in the CIE 1976 u'-v' uniform chromaticity coordinate system. At $T_j=50$ °C the chromaticity point is 0.009 units away from the original point and at 80 °C it is 0.02 units shifted from the original point. This exceeds the tolerable deviation limit of 0.01 units commonly used in the lighting industry.[17] The LE increases with decrease in the intensity of the red emitter and it decreases with the redshift of the red emitter. The decrease in LE at higher junction temperatures can be understood as the result of competition between the above two effects in which the decrease in efficacy due to redshift dominates. At longer wavelengths, the sensitivity of the human eye is lower.

To maintain the original chromaticity coordinates of the white-light source the power of each individual LED should be adjusted. This adjustment changes the original power ratio between LEDs and thus changes the shape of the spectrum.

[1] D. Kirkpatrick, Proc. SPIE **5187**, 10 (2003).
[2] J. Tsao, IEEE Circuits Devices Mag. **20**, 28 (2004).
[3] A. Zukauskas, M. Shur, and R. Gaska, *Introduction to Solid-State Lighting* (Wiley, New York, 2002).
[4] D. Steigerwald, J. Bhat, D. Collins, R. Fletcher, M. Holcomb, M. Ludowise, P. Martin, and S. Rudaz, IEEE J. Sel. Top. Quantum Electron. **8**, 310 (2002).
[5] E. F. Schubert, *Light Emitting Diodes* (Cambridge University Press, Cam-

bridge, U.K., 2003).

[6] A. Zukauskas *et al.*, Proc. SPIE **5187**, 185 (2003).

[7] N. Narendran, N. Maliyagoda, L. Deng, and R. Pysar, Proc. SPIE **4445**, 137 (2002).

[8] N. Narendran and L. Deng, Proc. SPIE **4776**, 61 (2002).

[9] Y. L. Li, J. M. Shah, P. H. Leung, Th. Gessmann, and E. F. Schubert, Proc. SPIE **5187**, 178 (2003).

[10] W. Thornton, J. Opt. Soc. Am. **61**, 1155 (1971).

[11] CIE publication, *Method of Measuring and Specifying Color Rendering Properties of Light Sources*, 13.3 (1995).

[12] J. C. Dyment, Y. C. Cheng, and A. J. SpringThorpe, J. Appl. Phys. **46**, 1739 (1975).

[13] Y. Gu and N. Narendran, Proc. SPIE **5187**, 107 (2003).

[14] S. Todoroki, M. Sawai, and K. Aiki, J. Appl. Phys. **58**, 1124 (1985).

[15] Y. Xi and E. F. Schubert (unpublished).

[16] T. Takeuchi, S. Sota, M. Katsuragawa, M. Komori, H. Takeuchi, H. Amano, and I. Akasaki, Jpn. J. Appl. Phys., Part 1 **36**, 382 (1997).

[17] A. Duggal, in *Organic Electroluminescence*, edited by Z. Kafafi (Marcel Dekker, New York, 2004).